International Journal of Signal Processing, Image Processing and Pattern Recognition
Vol.8, No.10 (2015), pp.401-412
http://dx.doi.org/10.14257/ijsip.2015.8.10.39

Aero-engine Vibration Signal Blind Separation Based on BP Neural Network Algorithm

Chen Yu*, Wen Xinling and Liu Zhaoyu

Zhengzhou Institute of Aeronautical Industry Management, Zhengzhou 450015, China
chenyu3440@gmail.com & wenxinling@zzia.edu.cn

Abstract

The normal running of the aero-engine is an important guarantee to the aviation aircraft flying in safe. As a result, the analysis and processing of the aero-engine vibration signal is an important task, which can realize the running state monitoring and fault diagnosis to the aviation aircraft. Due to the complexity of the aero-engine's structure, the vibration signals of aero-engine from the sensors fixed upon the aero-engine's brake often consist of several signals in aliasing, and also contain noise and other disturbance signal among them. The traditional vibration signal processing methods aiming at the anti-interference and de-noising have no significant effect. In addition, due to the non-linearity of the mixed signal, signal feature recognition and extraction is difficulties. This paper presented an application of the BP neural network to the aero-engine vibration signal separation, through the simulation of the aero-engine vibration signal induced by the high pressure rotor and low pressure rotor rotational imbalance; we proved the accuracy of the algorithm, which can separate the aero-engine vibration signal effectively. Through comparing with the fault spectrum characteristics of the aero-engine, the method can predict and diagnosis the aero-engine fault, which has a very important practical value.

Keywords: *Aero-engine; vibration signal; blind separation; BP neural network; learning algorithm*

1. Introduction

The aero-engine vibration signal is the important basis of detecting the aero-engine running state and fault diagnosis. The actual acquisition vibration signals is made up of the transmission system, such as different excitation sources of vibration signal aliasing, also contains the measurement noise and other disturbance signal, which brought difficulties to signal identification and fault diagnosis [1]. In this paper, we used the BP neural network method to separate the high/low pressure rotor vibration signals of the aero-engine according to the different sources signal. Through simulating the vibration signal of the fundamental frequency and the multiple frequency doubling signal due to the imbalance of the high and low pressure rotor of the aero-engine, we use the BP neural network method proposed in this paper on the rotor vibration signal and noise signal to realize separation verification, which proved the role of aero-engine vibration signals separation. After separating the aero-engine vibration signals effectively, we adopted the fault characteristic frequency to understand the running state of the aero-engine in time, which ensured the aircraft flight safety [2].

ISSN: 2005-4254 IJSIP

2. Structure and Fault Diagnosis of the Aero-engine

2.1. Structure of the Aero-engine

The moving parts of the double rotor aero-engine are mainly includes: the high pressure rotor (blade, disc, and shaft), low pressure rotor (blade, disc, and shaft), and other moving parts (including the drive gear, bearing, and pumps, etc.). [3-4] The high/low pressure rotor respectively is concentric shaft structure, the high pressure rotor is the outer shaft, and the low pressure rotor is the inner shaft, with the two rotor respectively running in different speed. The structure of two rotor aero-engine is shown in Figure 1.

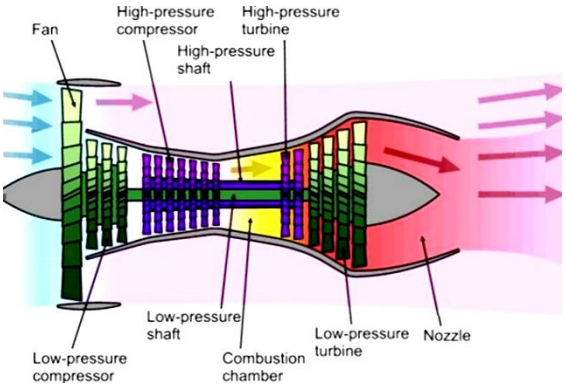

Figure 1. The Structure of Double Rotor aero-engine

2.2. Vibration Signal Monitor

Vibration signal is the important parameter to complete the fault diagnosis of aero-engine running state. When acquiring the vibration signal of the dual rotor engine, the sensors will be installed upon the engine's brake. Measured vibration signals are produced by the different aliasing signal, such as the high pressure rotor, low pressure rotor, and the transmission system, and also contain the measurement noise, etc. Separating the vibration signals in different excitation source, is the key step in the running state monitoring and fault diagnosis [5-6].

The traditional methods of the state signal analysis and feature extraction for the aero-engine mainly include: signal amplitude domain analysis, time-domain analysis, spectrum analysis based on Fourier transform, wavelet analysis, time-frequency analysis and modern spectral analysis, etc. These methods basically meet the requirements of the engineering practice, which played a huge role in the mechanical fault feature extraction. However, in practical engineering, the state monitoring and fault diagnosis system is widely used in the multiple point, multiple sensor collection mode. In the vibration test of the aero-engine, the vibration sensors are usually installed upon the outside of the engine brake. There are mechanical damping between the vibration source of aero-engine rotor, blades, gears, bearing and he engine brake, and the vibration propagation from the different vibration source spreads in various forms through the connecting structure, so, the signals that sensor collected an not directly reflect the actual situation of the vibration source, but the complex mixed signal produced by the different source. It brought difficulties to the signal identification and fault diagnosis.

2.3. Fault Analysis of Aero-engine Rotor

Although the aero-engine vibration problem is very complex, and the causes of vibration may be varied, it has a trace to be found. In the research of aero-engine vibration, researchers often classify the vibration sources as their structures, which is

divided into the main rotor vibration, blade vibration, bearing, etc. We examining the amplitude and energy of the fundamental frequency and every harmonic in order to find the source of vibration and carry out the troubleshooting. Part of the common failure of the double rotor turbofan aero-engine and their spectrum characteristics are listed as follows:

2.3.1. Rotor Imbalance: Due to the uneven of internal material's character, structural asymmetry, processing error and the rotor assembly error, the rotor's eccentric mass is bigger. In addition, the rotor has the circumstance of static bending, rotor hot bending, and rotor misalignment is wrong, all these can produce larger unbalanced vibration. Its frequency spectrum diagram expressed the peak value of the fundamental frequency is significantly higher than the peak value of the double and other fractional frequency.

2.3.2. Rotor Misalignment: The high pressure and low pressure rotor often appears deviation during the assembly process. Axis misalignment deviation is caused by the different bearing heart center shaft deflection among the adjacent bearing pedestal. The peak value of double frequency signal or multiple times' frequency is higher than the peak of fundamental frequency from the vibration signal spectrum diagram.

2.3.3. Rubbing between Rotor and Static Component: During the running process, because of the imbalance, small space between the rotor and static component, etc, which produce the vibration aggravation. The vibration features because of the rubbing is as follow: [7] In the early period of the rubbing fault, it will occur in part of the circle with obviously nonlinear vibration, this phenomenon will inspire high order harmonic component nf ($n = 1, 2, 3, 4, 5, \cdots\cdots$). When the rubbing is serious and the friction has spread throughout the circle, the rotors will have produced additional supporting effect and the high frequency vibration reduced gradually, the rubbing state of the fundamental frequency will become outstanding, this phenomenon will cause vibration of each frequency composition nf ($n = 1/2, 1/3, 1/4, 1/5 \cdots\cdots$).

2.3.4. Other Faults: There are blade vibration fault and bearing vibration fault, etc. For the turbofan engine, the important reason of the fan blades vibration is because the air flow induced by a kind of elastic mechanics involved in the field of pneumatic discussion of the vibration phenomenon-flutter. But the flutter phenomenon seldom occurs. Bearing vibration fault is about 30% among the aero-engine fault. Especially under the work circumstance of heavy load, high speed of aero-engine bearing, many fault such as fatigue wear peel, ablation, plywood, rust will appear.

3. Artificial Neural Network

Artificial Neural Networks (ANN) is an abstract description to the brain nervous system of the person or other biological, with same as the real nervous system. The artificial neural network can learn from the surrounding environment, change their behavior of the system by learning in itself, provide the effective ways to solve complicated problems, and realize the automatic control. The artificial neural network is the structure and function of the human brain neural system and the theory abstraction of the several basic characteristics, simplification and simulation, which is a kind of adaptive dynamic system consisted of a large number of neurons through the extremely rich and perfect connection [8]. Each neuron can be seen as a small processing units, these neurons are in some way connected each other, and make up of a neural network. The strength among the neurons connection can adaptive changes according to the stimulation of external signal, and each neuron can express excitement or dampening state with the combination size of multiple excitation signal received. The learning process of networks

is the process of adaptive change for the connection strength between neurons with the extrinsic information varying. For the Neural network self-learning and adaptive ability, it can analyze and grasp the potential regular though a number of input data and output data corresponding each other, and analyze and calculate the output result according to these regulars and the new input data. This study analysis process is known as "training", so, it has strong self-learning and image function with less manual intervention, has high precision with less use of expert knowledge.

3.1. Neurons Basic Structure Model

In artificial neural network, the most basic unit is the artificial neurons. [9] The artificial neuron is equivalent to a nonlinear threshold component with multiple input and output. The mathematical model of neuron structure is shown in Figure 2.

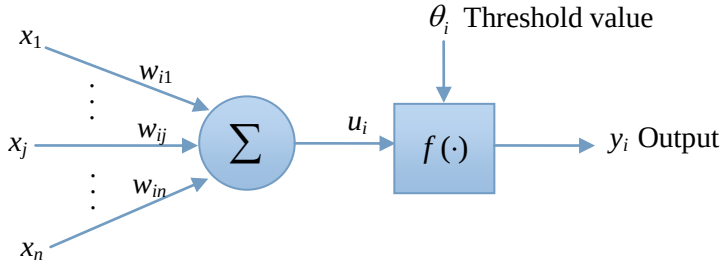

Figure 2. Artificial Neural Neurons Model

We can use the general mathematical expression to describe the operation of neurons *i*. The sum connects is the output of the linear accumulator, given the formula (1) as bellow:

$$u_i = \sum_{j=1}^{n} w_{ij} x = \boldsymbol{w}_i \boldsymbol{x} = \boldsymbol{x}^T \boldsymbol{w}_i \tag{1}$$

In formula (1), x is input signal vector, $w_i=[w_{i1},w_{i2},...,w_{in}]$ is weight of neurons *i*. The output of activation function is:

$$y_i = f(u_i - \theta_i) \tag{2}$$

Combining the formula (1) and (2) we can get the neurons output formula (3).

$$y_i = f(\sum_{j=1}^{n} w_{ij} x_j - \theta_j) \tag{3}$$

In the mathematical model of neurons, the activation function can be linear or nonlinear, in practice, we choose a different activation function according to the problems needing solved based on neural network.

3.2. BP Neural Network

BP neural network is multiple layer feed forward neural network based on error back propagation algorithm, each neuron only feed forward to the next layer of all neurons without the coupling in the layer, coupling and feedback coupling of every layer. Back propagation network is a multiple layer network that carries out the weight training to the nonlinear differential weights function. BP network includes the essence part of the neural

network theory, due to its simple structure, high plasticity; it has been widely used in many fields. Especially with the clear mathematical meaning and process steps, the learning algorithm has been more widespread application prospects.

Multiple layer BP neural networks not only have input nodes but also has output node, and there is one layer or multiple layer hidden nodes. Three layer of BP neural network topology is shown in Figure 3. This is basic structure with one input layer, one output layer, and one hidden layer. Each neuron connects with the next layer of all neurons, and each same layer neurons has no connection among them. In Figure3, the arrows indicate the flow of information.

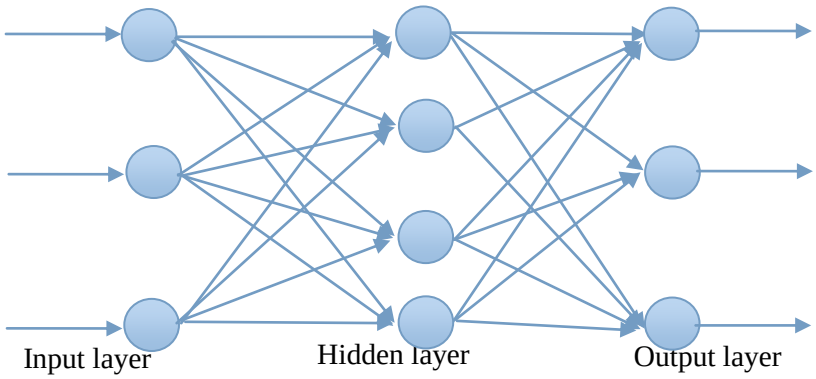

Figure 3. Topology Structure of Three layer Neural Network

Because the Sigmoid function has nonlinear amplification factor function, it can transform the input signal between minus infinity and plus infinity become an output with the value [-1, l]. To the larger input signal, the amplification coefficient is small, on the contrary, the smaller input signal, and amplification coefficient is larger. Because of the continuous and different nature of the sigmoid function, it has been more widely used in many data processing fields. So, BP neural network adopts the sigmoid activation function, which can go to process and approach the nonlinear relationship between the input and the output.

3.3. BP Network Learning Process

The production of the BP neural network is contributed with the BP neural algorithm; the BP algorithm belongs to the δ algorithm, which is a kind of supervised learning algorithm. And its main idea is: input for $\boldsymbol{q}$ learning samples $\boldsymbol{P^1}$, $\boldsymbol{P^2}$, ... , $\boldsymbol{P^q}$, and the corresponding output samples for $\boldsymbol{T^1}$, $\boldsymbol{T^2}$, ... , $\boldsymbol{T^q}$. The purpose of learning is to modify its weight by using the error between the actual output of the network $\boldsymbol{A^1}$, $\boldsymbol{A^2}$, ... , $\boldsymbol{A^q}$ Vector and the target vector of $\boldsymbol{T^1}$, $\boldsymbol{T^2}$, ... , $\boldsymbol{T^q}$, which makes vector A as close as the expected vector of $\boldsymbol{T}$.

BP algorithm is composed of two parts: the information positive transfer and the error back propagation. In the forward propagation, the input information calculated every layer from the input, the implicit layer to the output layer, the neurons state of each layer only affects the neurons state of the next layer. If the expected output can't be gotten in the output layer, the error varying value should be calculated, then turned back propagation to adopt the error signal to modify the weight of each neurons through reverse propagation of original network path, until get the desired goal. We make 3th layers BP network model as an example, the algorithm is listed below.

Set input node: x_j (j=1, ... , r), hidden node: y_i (i=1,...,$s1$), output node: O_k (k=1, ... , $s2$). The network weight value between the input node and the hidden node is $w1_{kj}$, and the network connection weight value between the hidden node and output node is $w2_{kj.}$ The

desired output is t_k. The activation function of the hidden layer is $f1(\cdot)$, the activation function of the output layer is $f2(\cdot)$。 [10][11]

3.3.1. The Positive Propagation of Information. (i) The output of i^{th} neurons in hidden layer is:

$$y_i = f1(\sum_{j=1}^{r} w1_{ij} x_j - \theta 1_i), \quad i=1,2,...,s1 \tag{4}$$

(ii) The output of k^{th} neurons in output layer is:

$$O_k = f2(\sum_{i=1}^{s1} w2_{ki} y_i - \theta 2_k), \text{k=1,2,...,s2} \tag{5}$$

(ii) Define the error function is:

$$E = \frac{1}{2}\sum_{k=1}^{s2}(t_k - O_k)^2 \tag{6}$$

3.3.2. Calculate the Weight Value Varying and Error Back Propagation based on the Gradient Descent Method. (i) The weight value varying in output layer. The weight value from the i^{th} input to k^{th} output is:

$$\Delta w2_{ki} = -\eta \frac{\partial E}{\partial w2_{ki}} = -\eta \frac{\partial E}{\partial O_k} \cdot \frac{\partial O_k}{\partial w2_{ki}} \tag{7}$$

Among it, $\frac{\partial E}{\partial O_k} = \frac{1}{2}\sum_i -2(t_i - O_i) \cdot \frac{\partial O_i}{\partial O_k} = -(t_k - O_k)$

$$\frac{\partial O_k}{\partial w2_{ki}} = \frac{\partial O_k}{\partial net2} \cdot \frac{\partial net2}{\partial w2_{ki}} = f2' \cdot yi \tag{8}$$

$\Delta w2_{ki} = \eta(t_k - O_k) f2' y_i = \eta \delta_{ki} \cdot y_i$, $\delta_{ki} = (t_k - O_k) f2' = e_k f2'$, $e_k = t_k - O_k$

(ii) The change of threshold in output layer. The threshold from the i^{th} input to k^{th} output is:

$$\Delta \theta 2_{ki} = -\eta \frac{\partial E}{\partial \theta 2_{ki}} = -\eta \frac{\partial E}{\partial O_k} \cdot \frac{\partial O_k}{\partial \theta 2_{ki}} \tag{9}$$

Among it, $\frac{\partial E}{\partial O_k} = -(t_k - O_k)$

$$\frac{\partial O_k}{\partial \theta 2_{ki}} = \frac{\partial O_k}{\partial net2} \cdot \frac{\partial net2}{\partial \theta 2_{ki}} = f2' \cdot (-1) \tag{10}$$

$\Delta \theta 2_{ki} = \eta(t_k - O_k) f2' = \eta \delta_{ki}$, $\delta_{ki} = (t_k - O_k) f2' = e_k f2'$, $e_k = t_k - O_k$

(iii) The change of threshold in hidden layer. The weight value from the j^{th} input to i^{th} output is:

$$\Delta w1_{ki} = -\eta \frac{\partial E}{\partial w1_{ki}} = -\eta \frac{\partial E}{\partial O_k} \cdot \frac{\partial O_k}{\partial y_i} \cdot \frac{\partial y_i}{\partial w1_{ij}} \tag{11}$$

Among it, $\frac{\partial E}{\partial O_k} = \frac{1}{2}\sum_{k=1}^{s2} -2(t_i - O_i)\cdot\frac{\partial O_i}{\partial O_k} = -\sum_{k=1}^{s2}(t_k - O_k)$

$$\frac{\partial O_k}{\partial y_i} = \frac{\partial O_k}{\partial net2}\cdot\frac{\partial net2}{\partial y_i} = f2^{'}\cdot\frac{\partial net2}{\partial y_i} = f2^{'}\cdot w2_{kj} \tag{12}$$

$$\frac{\partial y_i}{\partial w1_{ij}} = \frac{\partial y_i}{\partial net1}\cdot\frac{\partial net1}{\partial w1_{ij}} = f1^{'}\cdot x_j \tag{13}$$

$\Delta w1_{ij} = \eta\sum_{k=1}^{s2}(t_k - O_k)\cdot f2^{'}\cdot w2_{ki}\cdot f1^{'}\cdot x_j = \eta\delta_{ij}\cdot x_j$, $\delta_{ij} = e_i\cdot f1^{'}$, $e_i = \sum_{k=1}^{s2}\delta_{ki}w2_{ki}$

(iv) The change of threshold in hidden layer. The threshold from the j^{th} input to i^{th} output is:

$$\Delta\theta 1_i = -\eta\frac{\partial E}{\partial O_k}\cdot\frac{\partial O_k}{\partial y_i}\cdot\frac{\partial y_i}{\partial\theta 1_i} \tag{14}$$

Among it, $\frac{\partial E}{\partial O_k} = -\sum_{k=1}^{s2}(t_k - O_k)$

$$\frac{\partial O_k}{\partial y_i} = \frac{\partial O_k}{\partial net2}\cdot\frac{\partial net2}{\partial y_i} = f2^{'}\cdot\frac{\partial net2}{\partial y_i} = f2^{'}\cdot w2_{ki} \tag{15}$$

$$\frac{\partial y_i}{\partial\theta 1_i} = \frac{\partial y_i}{\partial net1}\cdot\frac{\partial net1}{\partial\theta 1_i} = f1^{'}\cdot(-1) = -f1^{'} \tag{16}$$

$\Delta\theta 1_i = \eta\delta_{ij}$, $\delta_{ij} = e_i\cdot f1^{'}$, $e_i = \sum_{k=1}^{s2}\delta_{ki}w2_{ki}$

The interpretation of error reverse propagation is as follows: the fact process of error back propagation is to calculate the error e_k of the output layer, and then get δ_{ki}, which multiply the e_k with the first order derivative $f2^{'}$ of the output layer activation function. Due to the hidden layer doesn't directly give the target vector, so we can take the output layer δ_{ki} to carry out reverse propagation of the error, to calculate the varying value of weights $\Delta w2_{ki}$ of the hidden layer. We can calculate $e_i = \sum_{k=1}^{s2}\delta_{ki}w2_{ki}$, and the same, we can multiply the e_i with the first order derivative $f1^{'}$ to calculate δ_{ki}, in turn to calculate the varying value $\Delta w1_{ij}$ in the front layer. If the front also has hidden layer, the same method applied as before, until calculating the first layer with reversing-deriving the output error e_i from layer to layer.

3.4. Aero-engine Vibration Signal Separation Method

Aero-engine vibration signals are made by the high/low pressure rotor, noise and signal aliasing. We drawn a certain number of sample points from the blind mixed signal $x(t)$, the high/low pressure rotor and harmonic signal exists in the vibration blind mixed signal $x(t)$. It is not the linear relation between the harmonic signal $s(t)$ produced by the low pressure rotor and the blind mixed signal $x(t)$. We use BP neural network algorithm to analyze this kind of transformation. The network input $s(t)$ is the low pressure rotor harmonic signals. The BP neural network studies the nonlinear transform of the low-pressure rotor signal $s(t)$, which associated the blind mixed signal $x(t)$ with $s(t)$, and estimate the low pressure rotor component value of the network output. In order to solve the time-varying possibility, we build the frame operation, and divide the blind mixed

signal $x(t)$ and $s(t)$ into the frame in N number of samples point as per unit length, among the frame, there are P number overlap sample point, so, their i^{th} frame element can be expressed as formula (17) :

$$x_i(n) = x(i(N-P)+n) \quad s_i(n) = s(i(N-P)+n) \tag{17}$$

Among the formula (17), $0 < n < N-1$, $i \geq 0$, network input is low pressure rotor signal $s(t)$, and the desired output is blind mixed signal $x(t)$, but, in fact, the low pressure rotor signal $\hat{s}(t)$ contain its harmonic aliasing signal in the mixed signal. So, we select input vector of the BP network is data point of $s(t)$. The desired output is made up of the data point in $x(t)$. Then, we train the BP neural, study the map relationship between $x(t)$ and $s(t)$. We express the input and output vector in BP neural network by the data frame of $x(t)$ and $s(t)$. To the i^{th} frame, input vector is expressed by matrix S_i, and output vector is expressed by X_i. It is shown as formula (18).

$$\begin{aligned} S_i &= [s_i(0), s_i(1), ..., s_i(N-1)]^T \\ s_i(n) &= [s_i(n), s_i(n-1), ..., s_i(n-j)] \\ X_i &= x_i(n)[x_i(0), x_i(1), ..., x_i(N-1)]^T \end{aligned} \tag{18}$$

Among the above formula (18), the n[th] rows of S_i is a j d data points, its desired output is $x_i(n)$. The line of matrix Si is made up of the sequence S_i and its j numbers sample. We can carry out the network train after we have input vector S_i and desired output vector $x_i(n)$. Through network training, we can build the map relationship between input vector Si and $x_i(n)$, then produce a nonlinear transform $\hat{s}(t)$ of $s(t)$, which is the low pressure rotor signal component in blind mixed signal xi(n). According to the Figure 4, we make $x(t)$ subtract $\hat{s}(t)$, and get the estimated vector $\hat{f}_i$ of $\hat{f}(t)$. The system description is shown as Figure 4. From the aero-engine vibration blind mixed signal we can conclude that the vector valued $\hat{f}_i$ should be the high pressure rotor signals, noise signals and other form of mixed signals.

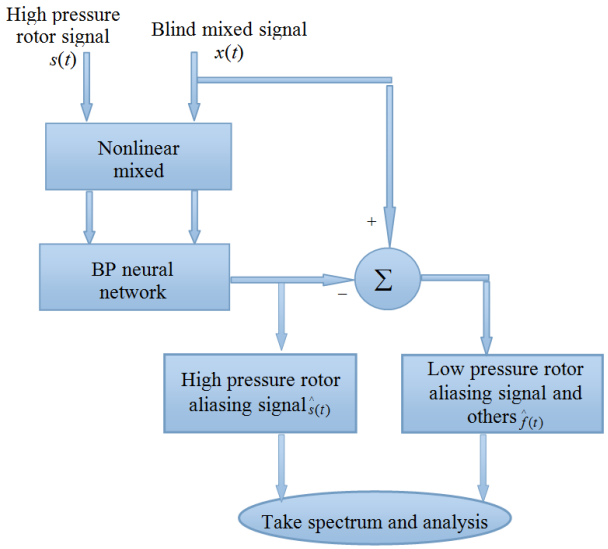

Figure 4. Aero-engine Vibration Signal Separation Frame

From the Figure 4 we can see, the low pressure rotor aliasing signal and other signals are gained through calculating as formula (19). We will carry out the spectrum to the separation signals and get the fault reasons through comparing the aero-engine fault character introduced in chapter 2.3.

$$\hat{f}(t) = x(t) - \hat{s}(t) \tag{19}$$

4. Experiment and Simulation

Some aero-engine vibration signal is collected by sensors fixed upon the engine brake. The vibration signal is produced by the high/low pressure rotor, and noise signal, etc. Suggest the speed or frequency of the high pressure rotor has been known, through the analysis before, we can get the vibration signal of the low pressure rotor and other signal. According to the aero-engine fault character, we suggest surface vibration signal on the brake because of the aero-engine high/low pressure rotor unbalanced. When this kind of fault appears, its vibration character express the fundamental frequency outstanding, and mixed by the multiple frequency signal, the peak of the multiple frequency signal is obviously less than the fundamental frequency. We simulate three groups of signal by the software of Matlab, respectively (i) fundamental frequency and multiple frequency signal (two times harmonic, and four times harmonic signals) of the high pressure rotor; (ii) fundamental frequency and multiple frequency signal (two times harmonic signal) of the high pressure rotor; (iii) noise and other interface signal. We blind mixed these three kinds of signals to simulate fact aero-engine vibration signal, and the blind mixed matrix is randomly selected, such as $\boldsymbol{A}$ as bellow.

$$A = \begin{bmatrix} 0.4447 & 0.6057 & 0.4564 \\ 0.6154 & 0.7382 & 0.3452 \\ 0.3453 & 0.4539 & 0.8798 \end{bmatrix}$$

We selected 4096 numbers of sample points of the blind mixed signals; the time-domain waveform diagram is show as Figure 5.

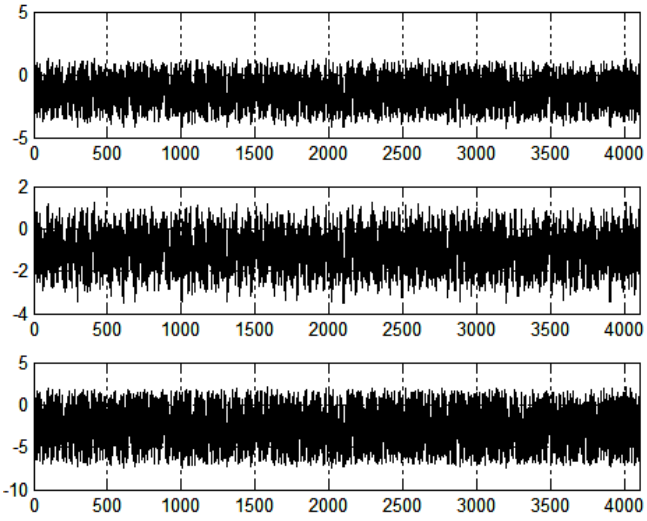

Figure 5. Blind Mixed Vibration Signal Waveform Diagram

From the blind mixed waveform diagram we cannot see the real source signal, and their spectrum are all chaotic, unable to distinguish the fundamental frequency and multiple frequency signal between high and low pressure rotor signals. The BP neural network chooses three layer network structures, the signal of the high pressure rotor

before 1000 points are acted as the sample points. And we carried out the feed-forward network training with the error performance target value of 0.001. After the BP neural network separation, the result is shown in Figure 6. Through the algorithm structure analysis in the Figure 4, theoretical, we should separate the fundamental frequency of the high pressure rotor and its double frequency, four times frequency aliasing signal, as well as the low pressure rotor fundamental frequency and double frequency signal, noise and other aliasing mixed signal.

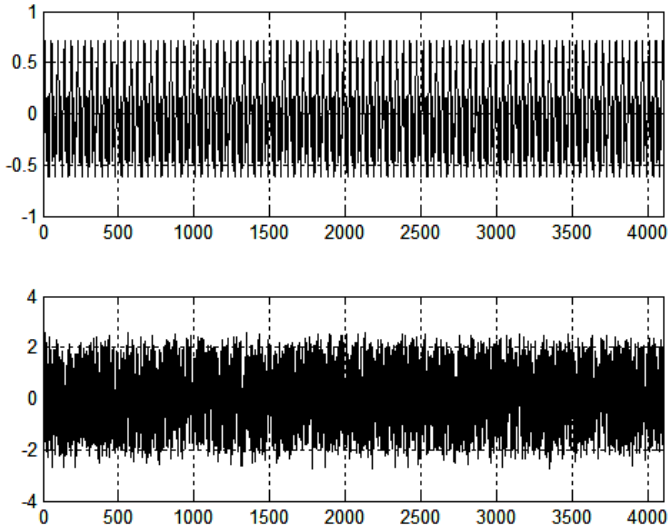

Figure 6. BP Neural Network Separation Signal Waveform Diagram

From the Figure 6 we still cannot see the character of the signal, so, we carried out the spectrum analysis to the separation signal. The spectrum result is shown as Figure 7.

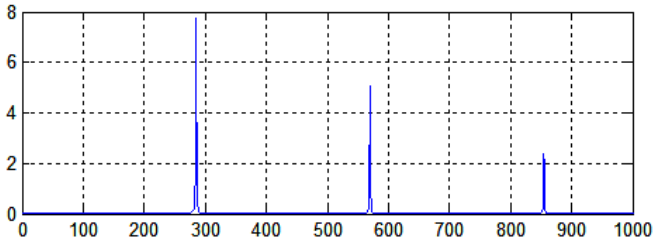

(a) The fundamental frequency and multiple frequency signal of the low.

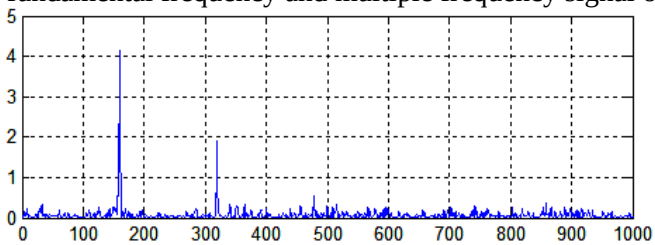

(b) The fundamental frequency, double frequency signal of the low pressure rotor, noise, and other interference signal.

Figure 7. BP Neural Network Separation Signal Spectrum Diagram

After separating the mixed signal by the BP neural, we take spectrum to Figure 6, and the result is shown as Figure 7, the Figure 7 (a) is the fundamental frequency and multiple frequency signal (double frequency and four times frequency) of the high pressure rotor, respectively is 285Hz, 569.8Hz, and 854.8Hz. Figure 7 (b) expressed the fundamental frequency and double frequency signal of the low pressure rotor signal (159.6Hz and

319.2Hz), noise, and other interference signal. Clear from Figure 7, the BP neural network algorithm this paper presented can separate high/low pressure rotor signal of the aero-engine accurately in the blind mixed signal, which can implement the aero-engine fault prediction and diagnosis.

5. Conclusion

The aero-engine vibration signal with noise is simulated by Matlab in this paper, and the aero-engine fault blind mixed vibration signal is separated based on the BP neural network algorithm. Through the simulation, the BP neural network algorithm can accurately show that the fundamental frequency, multiple frequency signals of the high/low pressure rotor and the noise interference signal can be obtain. When we understand any of the aero-engine rotating speed, such as high pressure rotor or low pressure rotor, we can act it as training signal, and get another signal including noise by BP neural network algorithm this paper presented. So, we can take the frequency spectrum to the separation signal to obtain the aero-engine fault accurately forecast based on the fault characters in order to guarantee the aviation aircraft flight safety, which has very important significance. In the future, we will use the actual aero-engine vibration signal to complete the separation practice, and improve the BP neural network algorithm to realize fault prediction and diagnosis on line.

Acknowledgements

This paper is supported by the Aviation Science Foundation Project (No. 2014ZD55007) and (No. 2014ZD55010), the research project of department of science and technology, Henan province (No. 132102210477), and science and technology research projects of Zhengzhou city technology bureau (No. 131PPTGG418-1).

References

[1] P. Jiang, M. Jia, F. Xu and J. Hu, "Feature Extraction of Weak Signal in Machine Fault Diagnosis", Journal of Vibration, Measurement & Diagnosis, vol. 25, no. 1, **(2005),** pp. 48-50.
[2] J. Ma, J. Chen and X. Liu long, "Application of Wavelet De-noising and Blind Source Separation in Aero-engine Fault Diagnosis", Computer Measurement & Control, vol. 11, no. 17, **(2009),** pp. 2115-2117.
[3] Z. Zhang, "Rotating Machinery Vibration Monitoring and Fault Diagnosis", Beijing: Mechanical Industry Press, **(1991)**, pp. 1- 203.
[4] D. Li and Y. Zhang, "Vibration Measurement and Test Analysis", Beijing: Mechanical Industry Press **(1992)**, pp. 370 -389.
[5] X. Song and M. Liao, "Vibration Signal Separation Techniques for Double-rotor Aero-engines", Mechanical Science and Technology, vol. 25, no. 4, **(2006),** pp. 487-496.
[6] J. Ma, Q. Shi, C. Cheng and S. Zhao, "Vibration Signal Separation Techniques in Aeroengine Test", Journal of Vibration, Measurement & Diagnosis, vol. 29, no. 1, **(2009),** pp. 1-4.
[7] L. Yang, K. Wang and Q. Zhang, "Whole body vibration condition evaluation of aero-engine on grey correlation degree", Journal of Shenyang Institute of Aeronautical Engineering, vol. 25, no. 5, **(2008),** pp. 9-11.
[8] D. Hebb, "The Organization of Behavior", New York, John Wiley & Sons **(1949),** pp. 86-97.
[9] M. T. Hogan, H. B. Demuth and D. Kui, "Neural Network Design", Beijing: Mechanical Industry Press, **(2006).**
[10] X. Yang and J. Zheng, Artificial" Neural Network and Blind Signal Processing", Beijng: Tsinghua University Press **(2003)**, pp. 32-35.
[11] Y. Chauvin and D. E. Rumelhart, "Backpropagation: Theory, Architectures and Applications", New York: Lawrence Erlbaum Associates Inc, **(1995)**.

Authors

Chen Yu, Association professor, he works at Zhengzhou Institute of Aeronautical Industry Management, Department of Electronic and Communication Engineering, research fields of circuit and system, data collection and signal process, network information and network security, etc.

Wen Xinling, Association professor, he works at Zhengzhou Institute of Aeronautical Industry Management, Department of Electronic and Communication Engineering, research fields of data collection and signal process, etc.